# Complexities in the climate of the subpolar North Atlantic: a case study from the winter of 2007

G. W. K. Moore,[a]* R. S. Pickart[b] and I. A. Renfrew[c]
[a]Department of Physics, University of Toronto, Ontario, Canada
[b]Woods Hole Oceanographic Institution, Massachusetts, USA
[c]School of Environmental Sciences, University of East Anglia, Norwich, UK
*Correspondence to: Prof. Kent Moore, University of Toronto, 60 St George Street, Toronto, Ontario, M5S1A7, Canada.
E-mail: gwk.moore@utoronto.ca

**As a result of its high topography, Greenland significantly distorts the atmospheric flow affecting local as well as remote weather systems and, via air–sea interaction processes, the coupled climate system. During February and March 2007, a field campaign was carried out to investigate this as part of the international Greenland Flow Distortion Experiment (GFDex). The observational programme occurred during anomalous conditions, relative to the climatological mean, that favoured the formation of barrier flow along the southeastern coast of Greenland and easterly tip jets at Cape Farewell, Greenland's southernmost point, while inhibiting the formation of westerly tip jets in the same region. The North Atlantic Oscillation (NAO) index was positive, indicating a deep Icelandic Low. However, there was a southeastward shift in the low's centre and a more zonally oriented storm track that we propose to be the result of the concurrent positive phase of the East Atlantic (EA) teleconnection. Unlike the usual situation for an NAO positive state, there was also a warming in the lower troposphere over the Labrador Sea that we argue was the result of a relatively weak Canadian Polar Trough over the eastern Canadian Arctic. It is shown that consideration of the strength of the Canadian Polar Trough in conjunction with information on the phases of the NAO and EA provides for a qualitatively better representation of the state of the atmosphere over the subpolar North Atlantic during the winter of 2007, and by inference in general, than is possible via the NAO alone. Copyright © 2011 Royal Meteorological Society**

*Key Words:* North Atlantic climate; North Atlantic Oscillation; East Atlantic mode; Baffin Island-West Atlantic mode

*Received 28 June 2010; Revised 16 November 2010; Accepted 21 December 2010; Published online in Wiley Online Library 23 March 2011*

*Citation:* Moore GWK, Pickart RS and Renfrew IA. 2011. Complexities in the climate of the subpolar North Atlantic: a case study from the winter of 2007. *Q. J. R. Meteorol. Soc.* **137**: 757–767. DOI:10.1002/qj.778

## 1. Introduction

The high topography of Southern Greenland results in significant flow distortion that leads to the common occurrence of high surface winds in the vicinity of Cape Farewell, its southernmost point. Indeed, a recent global climatology of surface marine winds identified this region as the windiest location on the ocean's surface (Sampe and Xie, 2007). Forecasters have been aware of this characteristic of the region for some time, and there is even evidence that these winds may have assisted in the Viking colonization of Greenland and Vinland (Renfrew *et al.*, 2008). The first description in the scientific literature of these winds was provided recently by Doyle and Shapiro (1999), who reported on the existence of an intermittent narrow region of westerly high surface wind speed, a phenomenon they referred to as a tip jet, that extended eastward from Cape Farewell. Moore (2003) developed the first climatology of high wind speed events near Cape Farewell. He found that the zonal wind in this region was bimodal with an increased probability of observing both westerly and easterly high-wind-speed events. Through a composite analysis, the westerly high-wind-speed events were found to be associated with tip jets of the type identified by Doyle and Shapiro (1999), while the easterly wind events represented a new phenomenon which Moore (2003) called 'reverse tip jets'. Subsequently it was proposed to distinguish between the two classes of Cape Farewell tip jets by the direction of the flow, i.e. westerly or easterly tip jets (Renfrew *et al.*, 2009a). We will adopt this convention in the present paper.

Both classes of wind events are associated with the interaction of synoptic-scale cyclones with the high topography of Southern Greenland. Westerly tip jets typically form when a synoptic-scale cyclone is situated in the lee of Cape Farewell between Greenland and Iceland, while easterly tip jets typically form when a synoptic-scale cyclone is situated to the south of Cape Farewell (Moore, 2003). In addition, Moore (2003) reported that westerly tip jets were more common during periods when the North Atlantic Oscillation (NAO) was in its positive phase, while easterly tip jets were more common in its negative phase. Bakalian *et al.* (2007) subsequently argued that the latitude of the centre of the Icelandic Low was also important in diagnosing westerly tip jet development, with these jets occurring more frequently when the low's centre was displaced northwards from its climatological mean position.

The intense air–sea interaction that is associated with these high wind speed events is important for both surface and deep ocean circulation and mixing in the region. For example, the surface wind stress in the vicinity of Southern Greenland plays a role in the forcing of the East Greenland Current and Coastal Current (Spall and Price, 1998) and the East Greenland Spill Jet (Pickart *et al.*, 2005), as well as in cyclonic recirculation gyres in the Irminger and Labrador Seas to the east and west of Cape Farewell, respectively (Lavender *et al.*, 2000; Spall and Pickart, 2003). In this regard, Doyle and Shapiro (1999) showed that there were large-momentum fluxes associated with a westerly tip jet event, while Martin and Moore (2007) showed the same applied to easterly tip jets. Doyle and Shapiro (1999) also noted that there were high fluxes of heat and moisture associated with the particular tip jet that they simulated. It has since been argued that these elevated heat fluxes are responsible for deep oceanic convection in the Irminger Sea (Pickart *et al.*, 2003; Våge *et al.*, 2008; Våge *et al.*, 2009). In the southeastern Labrador Sea, high heat fluxes associated with easterly tip jet events occur as well (e.g. Martin and Moore, 2007), but these appear not to be the norm, as demonstrated by Sproson *et al.* (2008). Winds along the southeast coast of Greenland, in the form of barrier winds (Moore and Renfrew, 2005; Petersen *et al.*, 2009), also frequently lead to elevated air–sea turbulent fluxes and these have been shown to be important for glacier melting through fjordic circulation changes (Straneo *et al.*, 2010) and modulating sea ice concentration (Dickson *et al.*, 1988). Confirmation of the importance of air–sea fluxes in driving the oceanic circulation in the region has been provided by Haine *et al.* (2009), who showed, through high-resolution ocean modelling experiments, that the resolution and magnitude of the wind forcing along with the fresh water flux due to precipitation are crucial for a realistic simulation of the surface mixed-layer development, current velocities and shelf-break volume fluxes along the southeast coast of Greenland.

Investigation of the flow distortion near Greenland has, until recently, relied mainly on global reanalysis products, surface wind speed retrievals from the QuikSCAT scatterometer and numerical weather prediction model output. The lack of *in situ* data with which to validate these remotely sensed data sources and model results has hampered our understanding of the structure and dynamics of these jets as well as their impact on the ocean. The Greenland Flow Distortion Experiment (GFDex) was proposed to improve this situation through the collection and analysis of *in situ* meteorological and oceanographic data. An overview of the experiment is provided by Renfrew *et al.* (2008) and the reader is referred to that publication for details on the observational plan and a summary of the data collected.

One unexpected aspect of the GFDex observational period, which occurred during late February and early March 2007, was the dearth of westerly tip jet events and the frequent occurrence of easterly tip jets (Outten *et al.*, 2009, 2010; Renfrew *et al.*, 2009a) – even though the NAO was in its positive phase. The NAO is associated with out-of-phase sea-level pressure anomalies between its two centres of action: the Icelandic Low and the Azores High. During its positive phase, the Icelandic Low is deeper than usual, while the Azores High is shallower than usual (Hurrell *et al.*, 2003; and see Figure 7(a) for an illustration). This regime is typically associated with enhanced storm activity over the North Atlantic, a northeasterly shift of the storm track, a high occurrence of cold-air outbreaks in the Labrador Sea and an increase in the occurrence of westerly tip jets, as well as a reduction in the occurrence of easterly tip jets (Hurrell *et al.*, 2003; Moore, 2003).

It must be emphasized, however, that the NAO explains only approximately 40% of the variance in the winter sea-level pressure field over the North Atlantic (Hurrell *et al.*, 2003). This suggests that there may be other circulation patterns that are important in characterizing the climate of the region. In this paper, we investigate the role that two additional teleconnections, the East Atlantic and Baffin Island–West Atlantic patterns, have on the anomalous conditions observed during the GFDex observational period as well as more generally on the climate of the subpolar North Atlantic.

The East Atlantic (EA) teleconnection was first identified in the empirical orthogonal function (EOF) analysis of Barnston and Livezey (1987). After the NAO, it is the leading mode of variability in the sea-level pressure field in the North Atlantic sector. It consists of a well-defined centre near 52.5°N, 27.5°W, with a more meridionally diffuse centre of the opposite phase over North Africa and the Mediterranean (Barnston and Livezey, 1987; Clinet and Martin, 1992; and see Figure 7(b) for an illustration). Its positive phase is associated with anomalously low sea-level pressure in the vicinity of its primary centre. Unlike the NAO, there has been relatively little research on the EA pattern and its impact on the climate. There is evidence that it modulates precipitation over southwest England and the Iberian Peninsula (Rodriguez-Puebla *et al.*, 1998; Murphy and Washington, 2001) as well as playing a role in the positioning of the primary North Atlantic storm track (Seierstad *et al.*, 2007; Woolings *et al.*, 2010). As one would expect, being the product of EOF analyses, indices of the NAO and EA are uncorrelated (Barnston and Livezey, 1987). During the GFDex observational period, we will show that both the NAO and EA were in their positive phase.

The so-called Baffin Island–West Atlantic (BWA) teleconnection was identified by Shabbar *et al.* (1997) through an EOF analysis of the winter mean 500 mb geopotential height field. They argued that this teleconnection provides information on the strength of the Canadian Polar Trough (CPT), the upper-tropospheric feature that is an important component of the stationary Northern Hemisphere winter wavenumber 3 pattern (Palmén and Newton, 1969; Held *et al.*, 2002; and see Figure 7(c) for an illustration). The BWA teleconnection is similar to the Western Atlantic teleconnection identified by Wallace and Gutzler (1981). Shabbar *et al.* (1997) suggested that a strengthening of the CPT that occurred around 1970 was responsible for the long-term cooling of the Labrador Sea region that started around that time. It is conventional in the literature to consider variability in the CPT as simply being the upper-level expression of the NAO (Hurrell *et al.*, 2003; Van den Dool *et al.*, 2006) and as such it is tacitly assumed that an index of the BWA contains no additional information. However, the correlation coefficient between the Jones *et al.* (1997) index of the NAO and a similarly defined index of the BWA during the winter months is approximately 0.7, indicating that variability in the NAO explains only 50% of the variance in the BWA. While this confirms that the two modes are related, there are likely situations where a consideration of the state of the BWA provides independent information on the climate of the subpolar North Atlantic that is not captured by the NAO alone. Indeed, as we shall show, the GFDex observational period was just such a situation; one during which the NAO and BWA were out of phase.

## 2. Methods

The National Centers for Environmental Prediction (NCEP) Reanalysis was one of the first reanalysis efforts to employ a frozen or time-invariant forecasting system to assimilate all available historical atmospheric and surface data (Kalnay *et al.*, 1996). It is available every 6 hours and covers the time period from 1948 to the present, with a horizontal resolution of approximately 2° at the surface and with 17 levels in the troposphere and stratosphere. With respect to the subpolar North Atlantic, Renfrew *et al.* (2002) showed that the NCEP Reanalysis was able to represent the observed synoptic variability during a 40-day ocean cruise in the Labrador Sea during the winter of 1997. Renfrew *et al.* (2009b) reached a similar conclusion with respect to the aircraft observations made during GFDex, although they emphasized that this global product was too coarse to capture the correct magnitudes of the mesoscale features present around Greenland, such as tip jets and barrier winds.

For the purposes of this paper, we have chosen to use the period 15 February to 15 March 2007 to characterize conditions during the GFDex observational period. Strictly speaking, the observations occurred between 21 February and 10 March 2007 (Renfrew *et al.*, 2008). However, no significant differences were found in mean conditions for these two slightly different time periods and so the longer period was chosen to provide a more robust climatology. Conditions during 2007 were compared to climatological values calculated over the same month-long time period based on data from 1948 to 2010.

The sea-level pressure field from the NCEP Reanalysis was used to compute indices of the NAO, the EA and the BWA for the period 15 February to 15 March, as well as for each of the winter months (December, January, February and March) for each of the years from 1948 to 2010. Following Jones *et al.* (1997), an NAO index was computed from the normalized sea-level pressure difference between Gibraltar (36.1°N, 5.3°W) and southwest Iceland (65°N, 22.8°W). For the months of February and March, the correlation coefficient between the instrumental NAO index of Jones *et al.* (1997) and the corresponding index derived from the NCEP Reanalysis was 0.98, confirming that the NCEP Reanalysis is able to capture the variability associated with the NAO. An index for the EA was computed as the normalized sea-level pressure anomaly at its primary centre at 52.5°N, 27.5°W (Murphy and Washington, 2001). As we will show, the NAO and EA indices that were derived in this way are uncorrelated. In similar fashion, an index for the BWA was computed using the 500 mb geopotential height field from the NCEP Reanalysis. Following Shabbar *et al.* (1997), centres of action over Bermuda (30°N, 60°W) and Baffin Island (65°N, 60°W) were used to compute this index. The centres used by Wallace and Gutzler (1981) in their definition of the Western Atlantic teleconnection are similar but not identical to those used by Shabbar *et al.* (1997). In addition, our BWA index differs from that used by Shabbar *et al.* (1997) so as to make it more consistent with and easier to compare to the NAO and EA indices; In particular, our BWA index is defined as the difference between the normalized anomalies in the 500 mb geopotential height field at the southern and northern centres of action. In contrast, Shabbar *et al.* (1997) defined their BWA index as one-half of the difference between unnormalized anomalies at northern and southern centres of action.

## 3. Conditions during 2007

Figure 1 shows the NAO, EA and BWA indices for the period 15 February to 15 March for each of the years from 1948 to 2010. As one can see, 2007 was characterized by positive values of the NAO and EA indices and a negative value of the BWA index. Figure 2 shows scatterplots of the EA and BWA indices against the NAO index for this period during each of the years from 1948 to 2010. As discussed above, the NAO and EA indices have a low degree of correlation that is manifested by the approximate equipartition amongst the four quadrants. The situation in 2007, in which the NAO and EA indices were both positive, occurs 27% of the time. In contrast, the NAO and BWA indices exhibit a higher degree of correlation, with the indices being of the same sign 76% of the time. More generally, these same approximate partitions also occurred during the months of December to March for the period 1948–2010 (not shown).

 

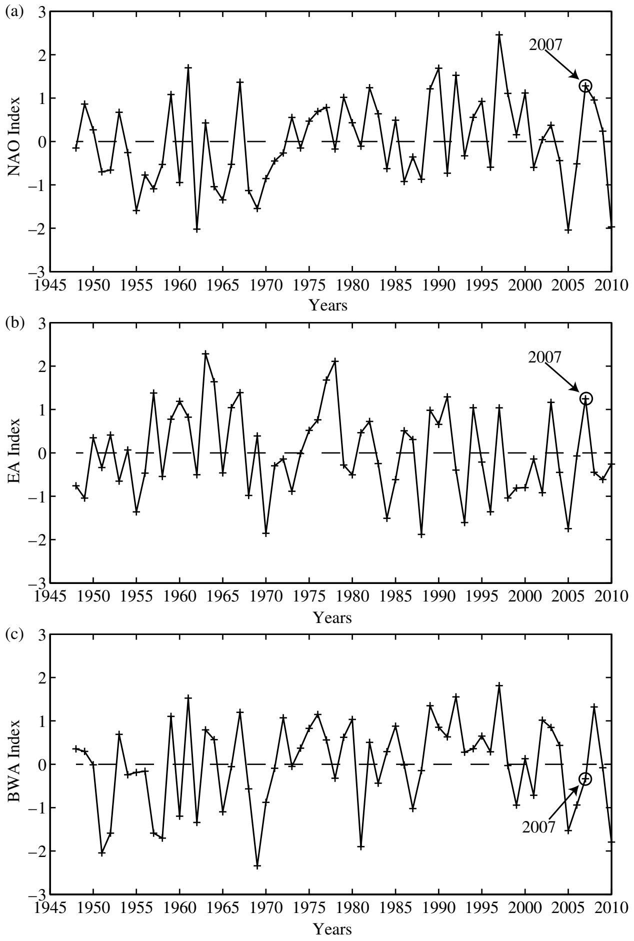


**Figure 1.** Indices of (a) NAO, (b) EA and (c) BWA teleconnection derived from the NCEP reanalysis during the period 15 February to 15 March for the years 1948–2010. For ease of comparison, all indices have been normalized to have unit standard deviation.

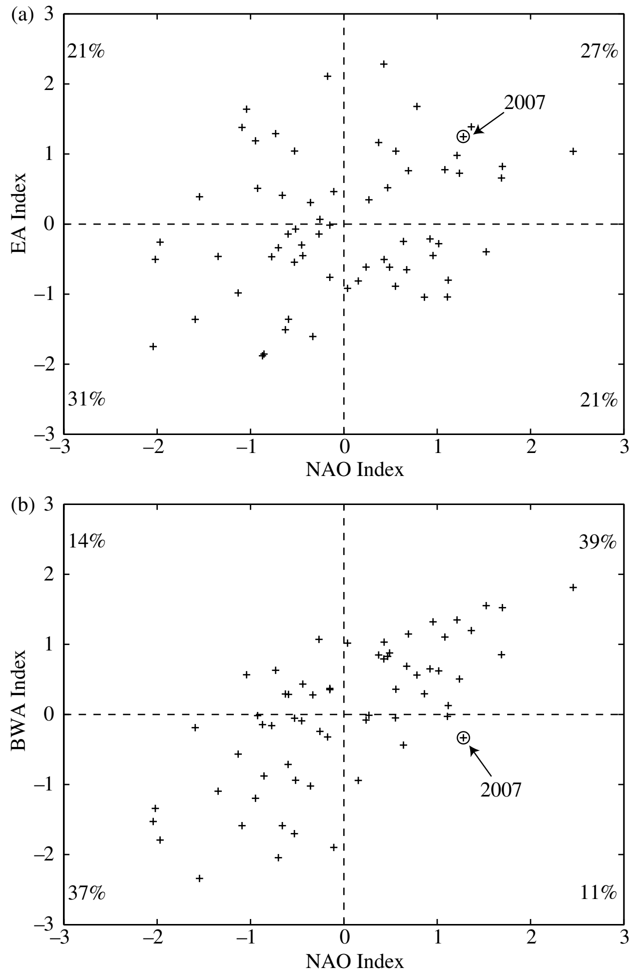


**Figure 2.** Scatterplot of NAO and (a) EA and (b) BWA indices derived from the NCEP reanalysis for the period 15 February to 15 March for the years 1948–2010. Also indicated are the percentage occurrences in each of the four quadrants defined by the sign of the two indices.

Figure 3 shows the mean-sea-level pressure field for the period 15 February to 15 March 2007 as well as the climatological mean of this field for the period 1948–2010 and the difference between the two. Consistent with the NAO index, one sees that the GFDex period was characterized by an increase in the meridional pressure gradient, with the central pressure of the Icelandic Low lowered from 1004 to 992 mb, while the central pressure of the Azores High increased from 1020 to 1024 mb. Note that there was also an anomalous region of high pressure over Hudson Bay during 2007 that contributed to an enhancement in the zonal pressure gradient over the Labrador Sea. The anomaly field (Figure 3(c)) clearly shows the southward movement of both the Icelandic Low and Azores High as well as the increase in pressure over Hudson Bay.

Figure 4 shows the corresponding 500 mb geopotential height fields. The dominant feature, the CPT, was weaker and had its centre displaced northwards in 2007 as compared to climatology. In addition, there were lower geopotential heights extending from the eastern seaboard of North America across to the British Isles and higher geopotential heights in the vicinity of the Cape Verde Islands. As a result, the geopotential height anomaly over the Eastern Canadian Arctic was out of phase with that in the vicinity of Iceland (Figure 4(c)).

Figure 5 shows the corresponding 1000–500 mb thickness fields expressed as temperatures. The figure indicates that over much of Eastern Canada and the subpolar North Atlantic the troposphere was warmer in 2007 as compared to climatology by up to 4°C over the Labrador Sea and Western Greenland. In addition, the troposphere over Western Europe was also warmer than climatology, while over the eastern seaboard of North America it was colder.

In Figure 6 we present a Eulerian diagnostic of synoptic-scale cyclone activity: the 2- to 6-day bandpass-filtered variance of sea-level pressure (Blackmon *et al.*, 1977). The location of regions of enhanced cyclonic activity are represented by high values of this field. During the 2007 GFDex period (Figure 6(a)), the storm track had a zonal orientation, with centres of high variance over the Great Lakes and to the south of Iceland just west of the British Isles. The climatological mean field (Figure 6(b)) shows that the storm track across the subpolar North Atlantic is typically oriented from the southwest to the northeast, extending from Newfoundland to Scandinavia. The anomaly field (Figure 6(c)) indicates that there was an increase in cyclonic activity over the western Great Lakes of North America, a reduction in cyclonic activity over much of the eastern North Atlantic northwards towards Greenland, as well as an increase in cyclonic activity to the south of Iceland extending eastwards towards the British Isles and Western Europe.

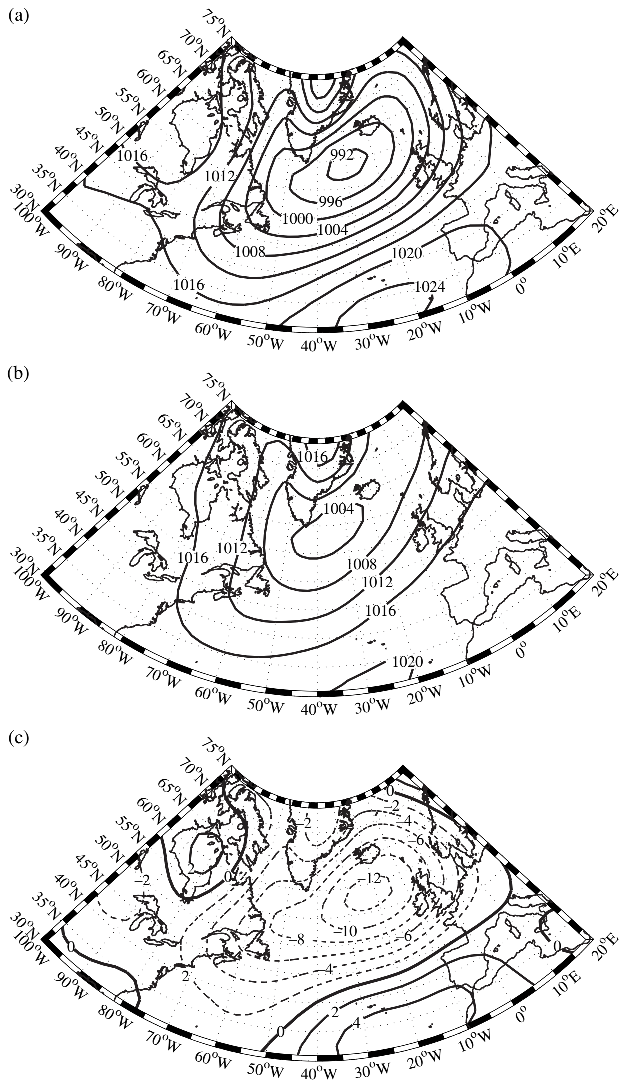


**Figure 3.** Sea-level pressure (mb) from the NCEP reanalysis for the period 15 February to 15 March for (a) mean conditions during 2007, (b) climatological mean 1948–2010 and (c) anomaly during 2007.

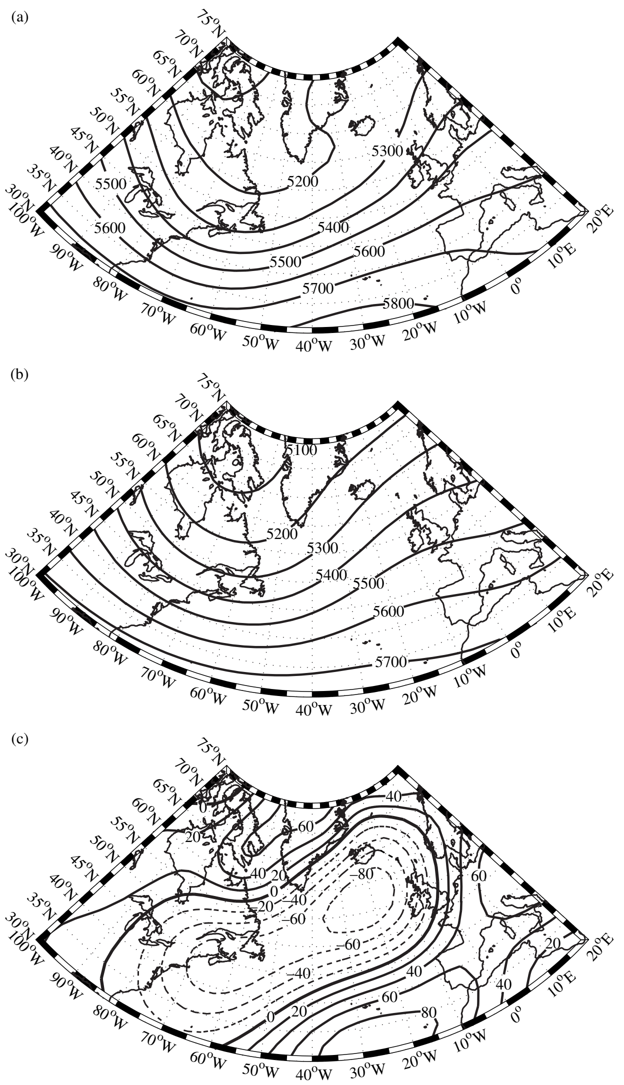


**Figure 4.** Geopotential height of the 500 mb surface (m) from NCEP reanalysis for the period February 15 to March 15 for (a) mean conditions during 2007, (b) climatological mean 1948–2010 and (c) anomaly during 2007.

To summarize, although February–March 2007 was a high-NAO period, its two centres of action were displaced to the south and the sea-level pressure anomaly over the Eastern Canadian Arctic was out of phase with that associated with the Icelandic Low. In addition, there was a more zonally aligned storm track with warmer temperatures over the Labrador Sea and Western Europe. These conditions are not typically associated with a positive NAO index.

## 4. Use of the NAO, EA and BWA to characterize conditions during 2007

In addition to being a high-NAO period, the GFDex months of February and March 2007 were also characterized by a positive value of the EA index and a negative value of the BWA index (cf. Figure 1). In this section, we seek to quantify and diagnose to what degree conditions observed during this period were anomalous as compared with those typically found when the NAO index is positive, and what additional information is gained by consideration of the variability in the EA and BWA teleconnection patterns. To accomplish this, a traditional composite analysis has been used to identify the atmospheric circulation patterns associated with positive and negative NAO conditions. In this case the composite is defined to be those winter months (December, January, February or March) during the period from 1948 to 2010 in which the magnitude of the NAO index was either positive or negative. Assuming a linear response, the difference between these two composites will be used to characterize the atmospheric response to the NAO (Wallace and Gutzler, 1981; Hoerling *et al.*, 1997). In a similar fashion, difference composites were created to characterize the atmospheric conditions associated with the EA and BWA teleconnections. The sign of the difference composites shown is that associated with a positive value of the respective index. These three difference composites, which will be referred to as 'NAOC,' 'EAC' and 'BWAC' respectively, will be compared to one generated for conditions during which the NAO and EA are of the same sign while the BWA is of the opposite sign – this is assumed to be representative of conditions during the GFDex observational period (cf. Figure 1) and which will be referred to as 'GFDexC'. Note the use of other thresholds for inclusion in the composites yielded similar results.

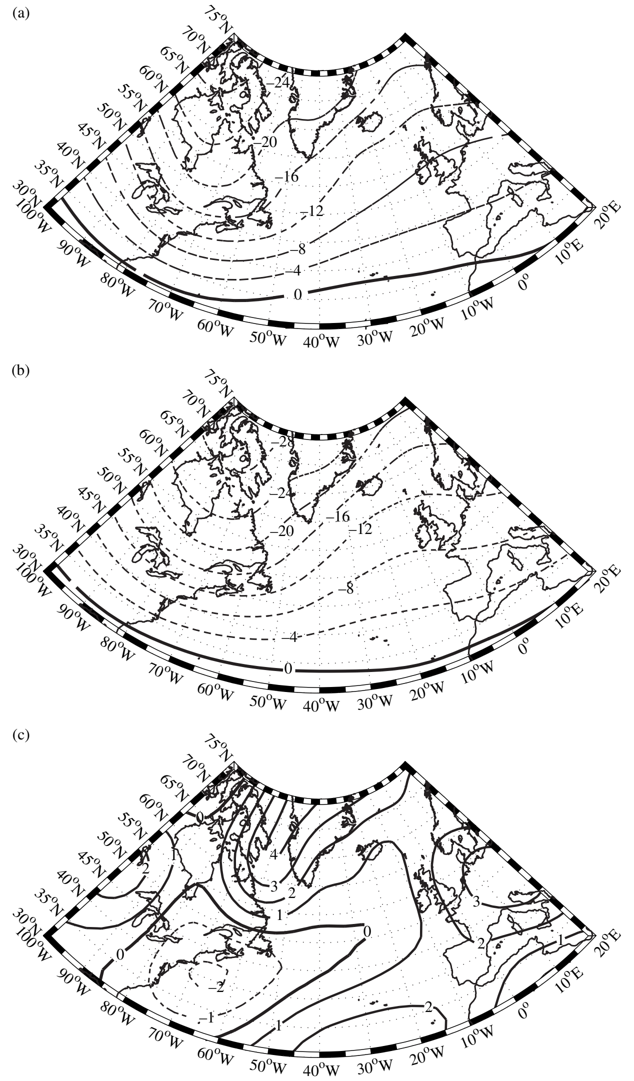


**Figure 5.** Thickness of the 1000–500 mb layer expressed as temperature (°C) from the NCEP reanalysis for the period February 15 to March 15 for (a) mean conditions during 2007, (b) climatological mean 1948–2010 and (c) anomaly during 2007.

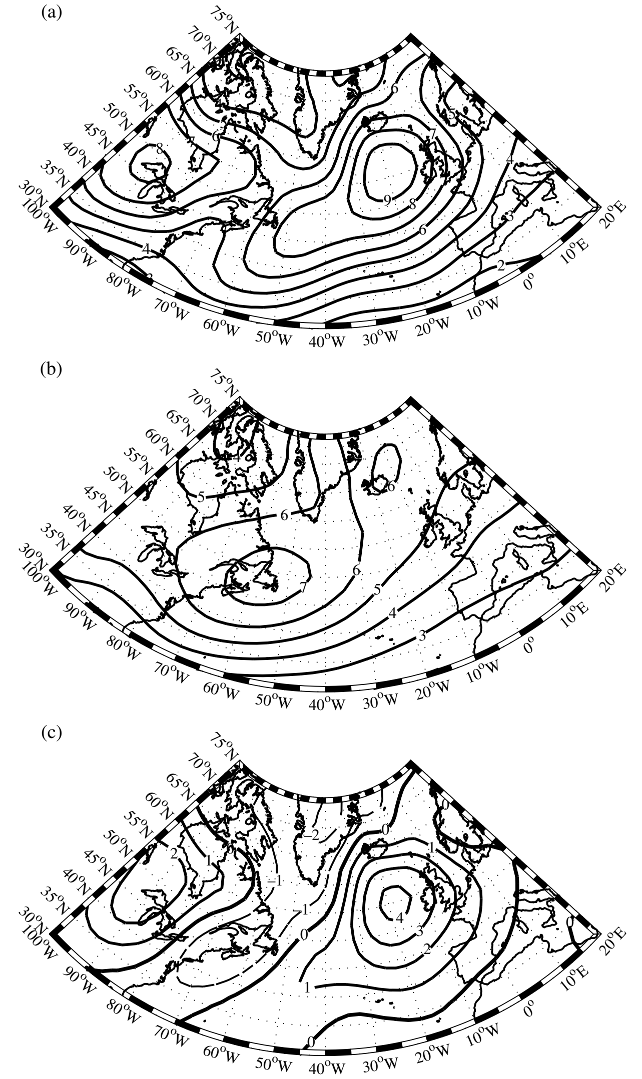


**Figure 6.** Bandpass 2- to 6-day filtered variance of the sea-level pressure expressed as standard deviation (mb) from NCEP reanalysis for the period February 15 to March 15 for (a) mean conditions during 2007, (b) climatological mean 1948–2010 and (c) anomaly during 2007.

Figure 7 shows the difference composites for the sea-level pressure field. The NAOC (Figure 7(a)) shows the conventional meridional dipole with a reduction in sea-level pressure near Iceland and an increase in pressure near the Azores (Hurrell *et al.*, 2003). The dipole extends zonally across the subpolar North Atlantic from Eastern North America eastwards to Europe and, in this case, the sea-level pressure in the Eastern Canadian Arctic is in phase with that near Iceland. The EAC (Figure 7(b)) shows a well-defined monopole with a centre to the south of Iceland and to the west of the British Isles (Barnston and Livezey, 1987). The BWAC (Figure 7(c)) shows a meridional dipole shifted westward from that associated with the NAO. The GFDexC (Figure 7(d)) shows a southwest-to-northeast aligned tripolar structure with higher sea-level pressures centred over the Hudson Bay and North Africa and lower sea-level pressures extending across the subpolar North Atlantic, with a southward displacement of both the Icelandic Low and Azores High. In addition for this case, the sea-level pressure anomaly in the Eastern Canadian Arctic is out of phase with that near Iceland. We would argue that this composite (Figure 7(d)) provides a considerably better representation of conditions during February–March 2007 (Figure 3(c)) than that provided by the NAOC (Figure 7(a)).

Figure 8 shows the analogous difference composites for the 500 mb geopotential height field. The NAOC (Figure 8(a)) is similar to that of the sea-level pressure composite (Figure 7(a)), with the exception of a slight westward shift in the two centres of action as compared to their locations at the surface. Clearly, when one considers just the NAO index, variability in the CPT is in phase with variability of the Icelandic Low. The EAC (Figure 8b) has the same monopole structure, also with a slight westward shift in its centre as compared to the situation at the surface (Figure 7(b)). The BWAC (Figure 8(c)) shows a well-defined dipolar structure with centres over Baffin Island and the southwest North Atlantic near Bermuda. The GFDexC (Figure 8(d)) has the same tripolar structure seen in the sea-level pressure field (Figure 7(d)). As a result, the 500 mb geopotential height anomaly over the Labrador Sea is out of phase with the sea-level pressure anomaly near Iceland. These characteristics are similar to those that occurred in February–March 2007 (compare Figure 8(d) to Figure 4(c)).

 

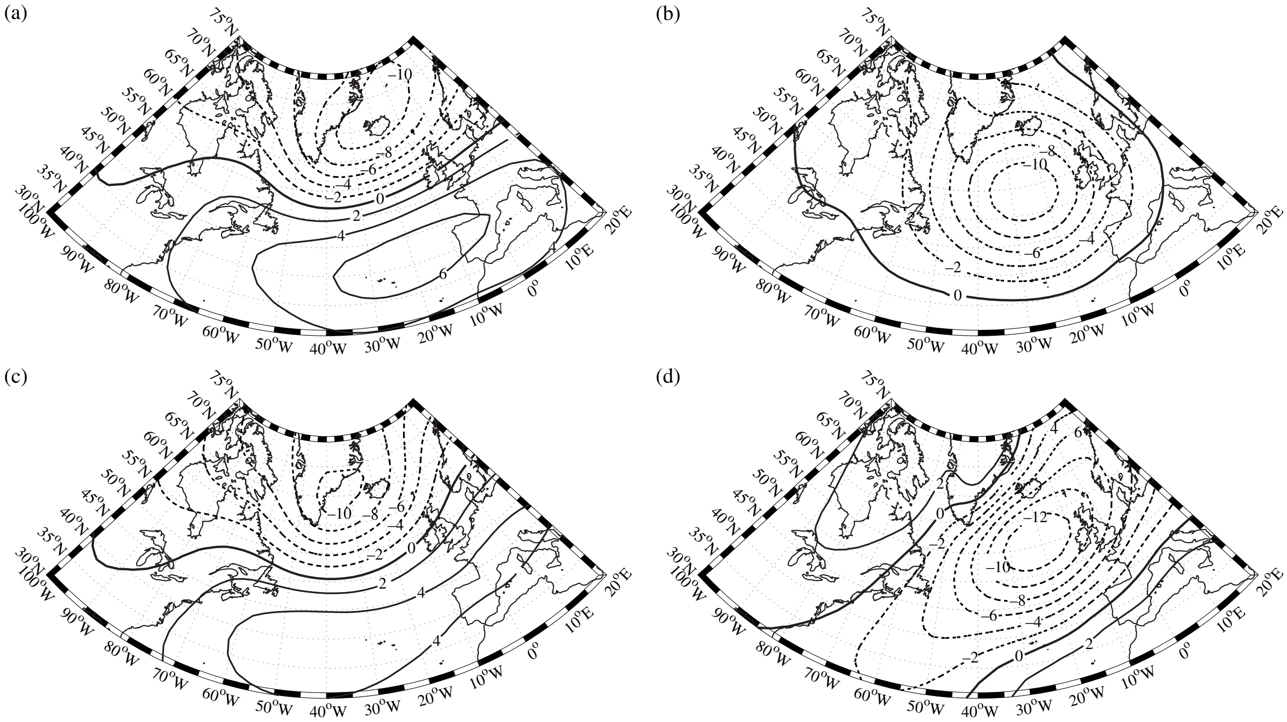


**Figure 7.** Composites of the mean-sea-level pressure (mb) from NCEP reanalysis for the winter months (DJFM) from 1948 to 2010 for (a) the NAOC case, (b) EAC, (c) BWAC and (d) the GFDexC case. See text for a description of the various cases.

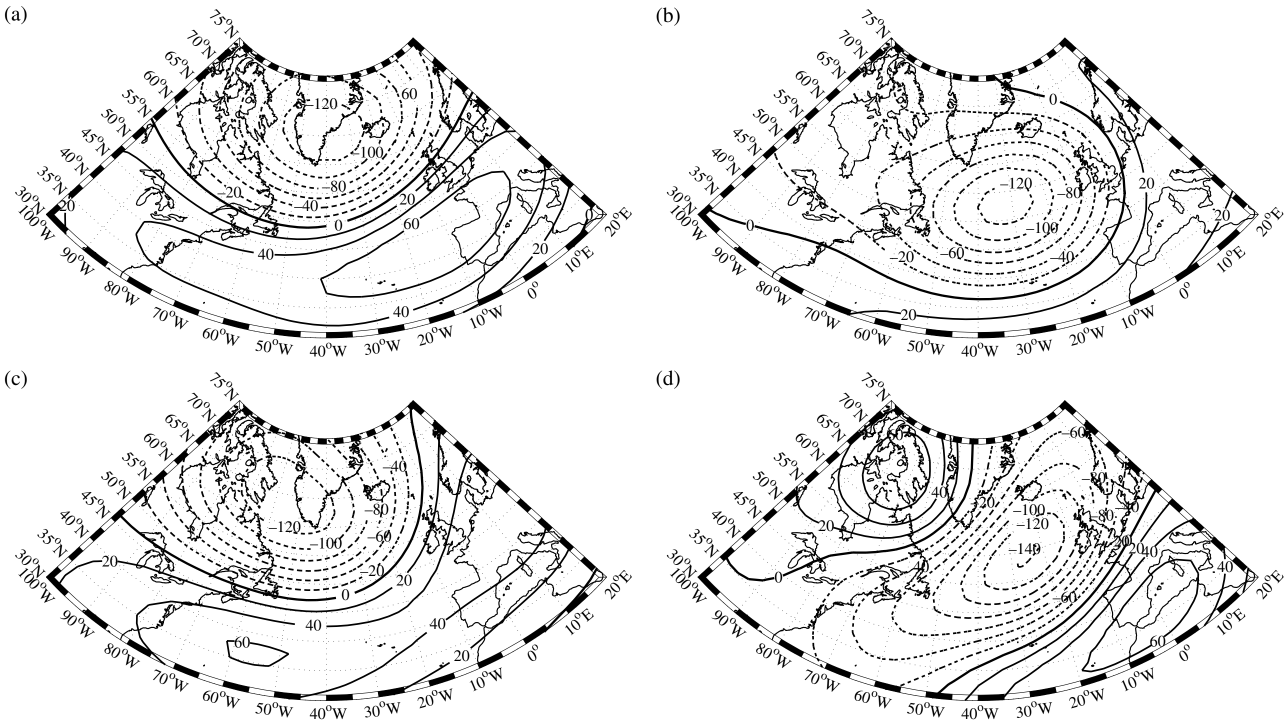


**Figure 8.** Composites of the 500 mb geopotential height (m) from the NCEP reanalysis for the winter months (DJFM) from 1948 to 2010 for (a) the NAOC case, (b) EAC, (c) BWAC and (d) the GFDexC case. See text for a description of the various cases.

Figure 9 shows the difference composites for the 1000–500 mb thickness field expressed as a temperature. The NAOC (Figure 9(a)) indicates that when the NAO index is positive it is colder in the troposphere over the Labrador Sea and across the subpolar North Atlantic to Iceland, with warmer tropospheric temperatures over Scandinavia and Europe. The EAC (Figure 9(b)) shows a similar zonally oriented dipole similar to that for the NAO (Figure 9(a)) except for a southward shift in its axis. The BWAC (Figure 9(c)) shows a similar pattern to that for the NAO (Figure 9(a)) except for southwestward movement of the cold anomaly over the Labrador Sea and an elongation towards the southeast. The GFDexC (Figure 9(d)) has a tripolar structure, similar to that seen in the corresponding sea-level pressure and 500 mb geopotential height composites (Figures 7(d) and 8(d)).

 

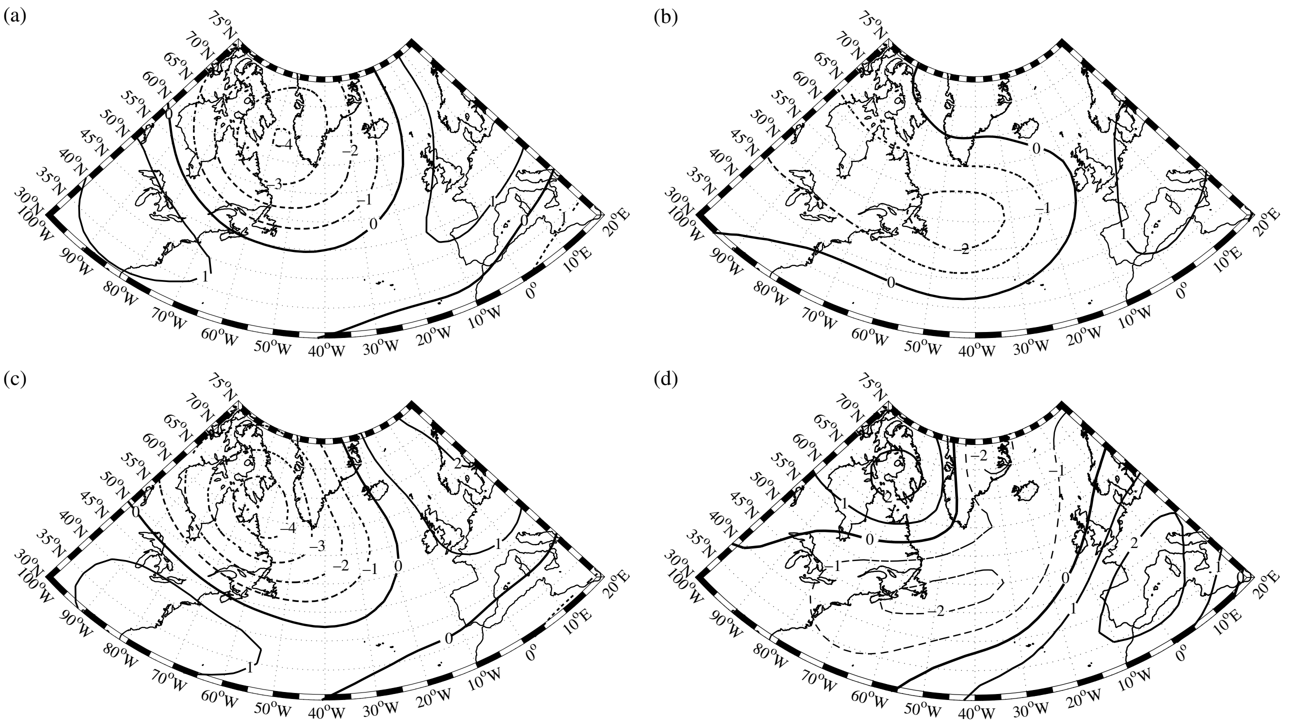


**Figure 9.** Composites of the thickness of the 1000–500 mb layer expressed as temperature (°C) from the NCEP reanalysis for the winter months (DJFM) from 1948 to 2010 for (a) the NAOC case, (b) EAC, (c) BWAC and (d) the GFDexC case. See text for a description of the various cases.

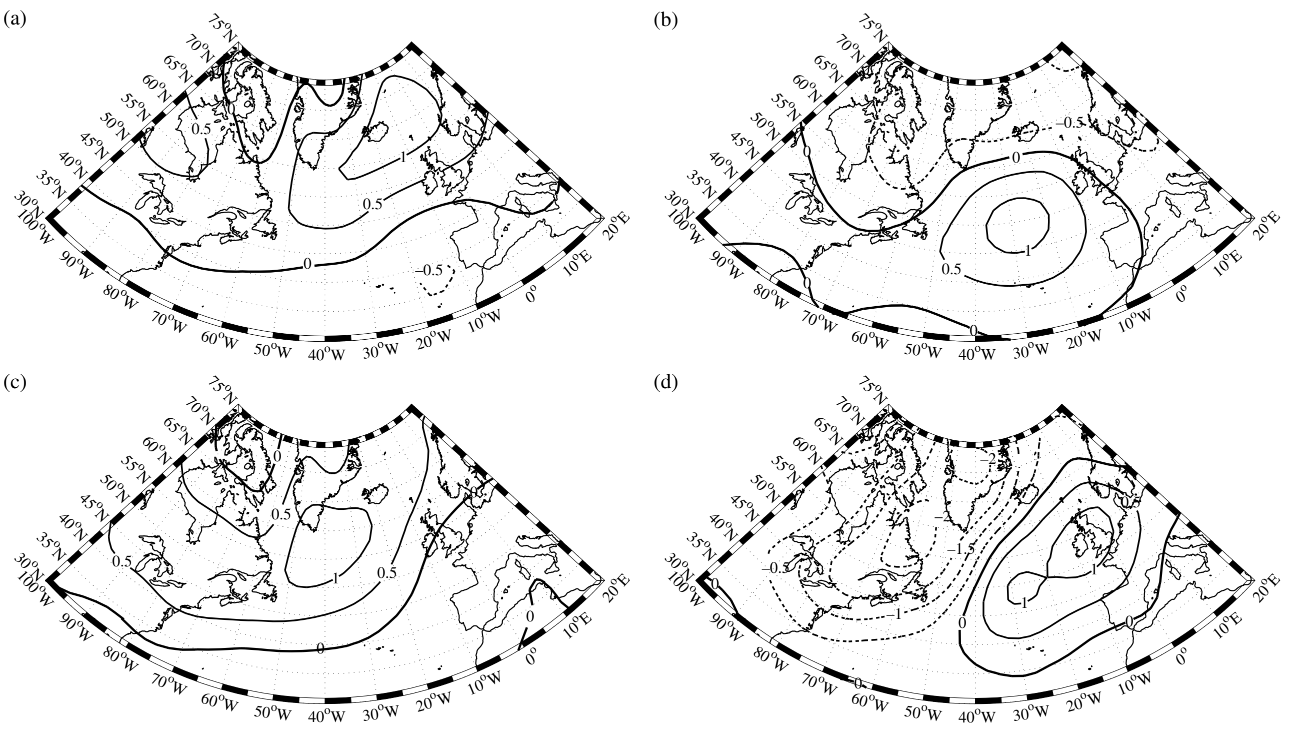


**Figure 10.** Composites of the bandpass 2- to 6-day filtered variance of the sea-level pressure expressed as standard deviation (mb) from the NCEP reanalysis for the winter months (DJFM) from 1948 to 2010 for (a) the NAOC case, (b) EAC, (c) BWAC and (d) the GFDexC case. See text for a description of the various cases.

We suggest that this composite (Figure 9(d)) represents conditions during February–March 2007, in contrast to the NAOC (Figure 9(a)). In particular, it captures the observed meridional dipole that extends from the Eastern Canadian Arctic to the Eastern Seaboard of North America, as well as the warming over Europe (Figure 5(c)). However it does not capture the warming over Scandinavia observed in 2007.

Finally, Figure 10 shows the difference composite anomalies for the 2- to 6-day bandpass-filtered variance of sea-level pressure. The NAOC (Figure 10(a)) indicates an increase in cyclone activity across much of the subpolar North Atlantic, extending northeastward from Newfoundland to Scandinavia. The EAC (Figure 10(b)) indicates an increase in cyclone activity to the south of Iceland and to the west of the British Isles, with a decrease in cyclone activity over the Eastern Canadian Arctic, Greenland and Scandinavia. The BWAC (Figure 10(c)) shows a northward shift in the storm track, with a maximum near Cape Farewell. The GFDexC (Figure 10(d)) shows a southwest-to-northeast oriented dipolar pattern, with an increase in cyclone activity extending from south of Iceland to the British Isles and a decrease in activity extending from the Eastern Seaboard of North America to Greenland. This pattern was also observed during February–March 2007 (Figure 6(c)).

To summarize, a composite of NAO-positive, EA-positive and BWA-negative conditions for the winter months provides a qualitatively accurate representation of the key features of the synoptic-scale circulation of February–March 2007 for the subpolar North Atlantic. In contrast, consideration of each of these circulation patterns in isolation does not.

## 5. Discussion

During any field programme one has a limited time in which to make observations and it is therefore important to describe the large-scale meteorological conditions during the data collection period in order to place the observations in their proper climatological context. This is especially true during an experiment such as GFDex, in which the processes under investigation have an impact on timescales much longer than that of the observation period. Although the NAO index was positive during the field phase of GFDex, surprisingly no westerly tip jets were observed (Renfrew *et al.*, 2008). As we have shown, the mean conditions during the field phase of GFDex were anomalous with regard to typical positive NAO conditions in that the centres of the Icelandic and Azores High were displaced southwards, the storm track was more zonally oriented, tropospheric temperatures over Greenland were warmer than usual and the CPT was weaker than usual. In terms of teleconnection indices, the NAO and EA indices were positive, while the BWA index was negative (Figure 1).

As we have shown in Figures 7–10, conditions that occur when the NAO and EA indices are of the same sign while the BWA index is of the opposing sign are markedly different from those that occur when one considers *only* the sign of the NAO index. In particular, the former situation results in the existence of tripolar anomalies in the mass field across the subpolar North Atlantic, with opposing signs in the anomalies situated to the west and east of Greenland, along with a southward migration of the Icelandic Low and the Azores High. Such opposing anomalies and the southward migration were key characteristics of the GFDex observational period (Figures 3(c)–6(c)).

Our analysis suggests that all three teleconnection patterns contributed to the anomalous conditions observed during the GFDex observational period as well as being required to fully capture the complexities of the climate of the subpolar North Atlantic. However, it is unclear what the individual contributions of the EA and BWA patterns are and whether both are necessary to adequately capture the complexities seen during the GFDEX observational period. Figure 11 shows the composite difference fields of the sea-level pressure and 1000–500 mb thickness fields for the case in which the NAO and the EA indices are of the same sign (irrespective of the BWA index) and the case in which the NAO and BWA indices are of opposing signs (irrespective of the EA index). The sea-level pressure composite for the case in which the NAO and EA indices are of the same sign (Figure 11(a)) when compared to the corresponding NAO composite (Figure 7a) clearly shows the southward migration of the Icelandic Low and Azores High that is the result of the consideration of the phase of the EA teleconnection pattern. In contrast, inclusion of variability in the BWA teleconnection pattern (Figure 11(b)) captures the dipolar nature of the sea-level pressure field present during the GFDex observational period, with conditions to the west of Greenland being out of phase with those to the east. The composite of the 1000–500 mb thickness field for the case in which the NAO and EA indices are of the same sign (Figure 11(c)) retains the structure seen in the NAO composite (Figure 9(a)) but with a southward migration in the anomaly over the Labrador Sea, whereas the corresponding composite for the case in which the NAO and BWA indices are of opposing sign (Figure 11d) has thermal anomalies of opposing sign to the west and east of Greenland.

It is therefore clear, qualitatively, that the combination of just these pairs of indices produces composites that do not match the February–March 2007 period as well as using all three indices (compare Figure 11 to Figures 3(c) and 5(c)). These results, however, do shed light on the relative contributions of the EA and BWA patterns to conditions observed during February–March 2007. In particular, the positive phase of the EA was responsible for the southward movement of the centres of action of the NAO, while the negative phase of the BWA was responsible for the warmer temperatures over the Labrador Sea.

In terms of atmospheric forcing of the ocean, Våge *et al.* (2009) showed that the winter of 2007 as a whole was characterized similarly to the GFDex period embedded within that winter, including: anomalously northeasterly flow in the Labrador and Irminger Seas; less tendency for storms to veer northeast towards Iceland; and fewer occurrences of westerly tip jets. In addition, we have shown that the lower tropospheric temperatures over the Labrador Sea were anomalously warm (Figure 5(c)). This resulted in weaker than normal air–sea heat fluxes in the Labrador and Irminger Seas, and consequently deep convection did not occur (Våge *et al.*, 2009; Yashayaev and Loder, 2009). This goes against the general notion that a high NAO index means enhanced overturning in the Labrador Sea (Marshall *et al.*, 1998; Dickson *et al.*, 2000; Pickart *et al.*, 2003). Interestingly, during the following winter deep convection did occur, even though the NAO index was lower than in the previous year. As seen from Figure 1, the BWA index became positive that year, resulting in cooling over the Labrador Sea (Figures 9(c) and 12), which in turn contributed to air–sea buoyancy fluxes that were favourable for convective overturning in both the Labrador and Irminger Seas (Våge *et al.*, 2009; Yashayaev and Loder, 2009).

## 6. Conclusions

Conditions during the GFDex observational period in late February and early March 2007 have been shown to be anomalous to what is usually expected when

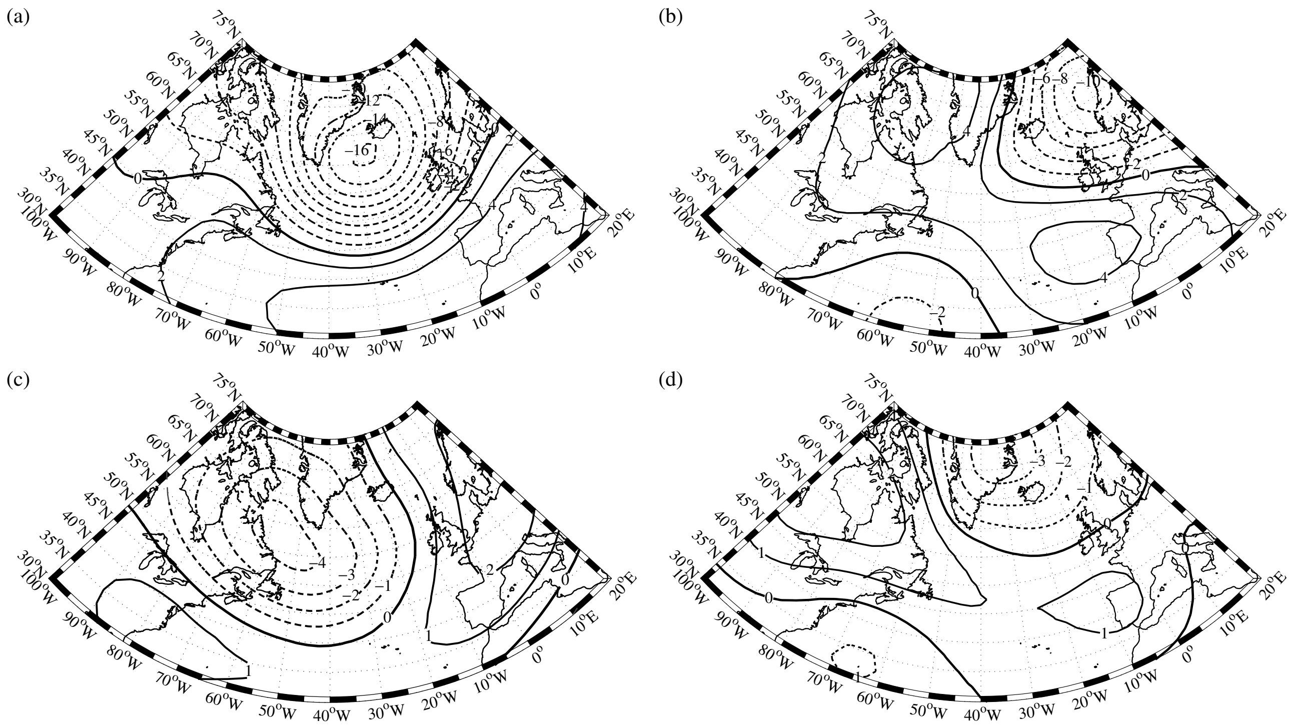


**Figure 11.** Composite of (a, b) mean-sea-level pressure (mb) and (c, d) 1000–500 mb layer expressed as temperature (°C) from NCEP reanalysis for the winter months (DJFM) from 1948 to 2010. Panels (a, c) represent the difference between months in which NAOI > 0 and EAI > 0 from those in which NAOI < 0 and EAI < 0. Panels (b, d) represent the difference between months in which NAOI > 0 and BWAI < 0 from those in which NAOI < 0 and BWAI > 0.

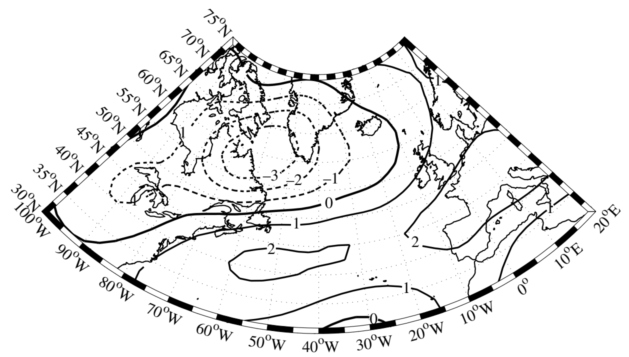

**Figure 12.** Anomaly in thickness of the 1000–500 mb layer expressed as temperature (°C) from NCEP reanalysis during the period 15 February to 15 March 2008.

the NAO is in its positive phase. These anomalous conditions included a southward shift in the centres of the Icelandic Low and the Azores High, as well as thermal anomalies over the Labrador Sea being out of phase with those near Iceland. This situation resulted in enhanced northerly flow to the east of Greenland, which led to more barrier wind and easterly tip jets events as well as an absence of westerly tip jet events (Renfrew *et al.*, 2008).

Through the consideration of two other teleconnection patterns – the East Atlantic (EA) and Baffin Island–West Atlantic (BWA) patterns – we have been able to demonstrate that the field phase of GFDex was associated with a situation in which the Icelandic Low was deeper than normal, i.e. the NAO index was positive; the centre of the Icelandic Low was shifted southwards from its climatological position, i.e. the EA index was positive; while the Canadian Polar Trough was weaker than usual, i.e. the BWA index was negative. Such conditions still lead to a dipolar sea-level pressure anomaly across the subpolar North Atlantic with characteristics that, as we have shown, are different from those that result from consideration of the variability in the NAO index alone.

Our results suggest that a more complete description of the climate of the subpolar North Atlantic also requires consideration of (1) the strength of the upper-level flow over the Eastern Canadian Arctic, as expressed in the BWA index; (2) the strength of surface flow (in other words the depth of the Icelandic Low and Azores High), as expressed in the NAO index; and (iii) the location of these centres, as expressed in the EA index. In addition, there may be other teleconnections, such as the Scandinavia pattern (Barnston and Livezey, 1987), that may also contribute to a complete description of the region. Finally, the relative magnitudes of the various indices also contribute to the structure of the anomaly for a given time and should also be taken into account.

## Acknowledgements

The authors would like to thank all the participants of the Greenland Flow Distortion Experiment (GFDex) for discussions that have contributed to this work. GFDex was funded by the Natural Environmental Research Council (NE/C003365/1), the Canadian Foundation for Climate and Atmospheric Sciences (GR-641), and the EUFAR (European Fleet for Airborne Research) and EUCOS (European Coordinated Observing System) schemes. RP was supported by grant OCE-0726640 of the National Science Foundation. The authors would like to gratefully acknowledge the suggestions provided by the reviewers that significantly improved the paper.

 

## References


Bakalian F, Hameed S, Pickart R. 2007. Influence of the Icelandic Low latitude on the frequency of Greenland tip jet events: implications for Irminger Sea convection. *J. Geophys. Res.* **112**: C04020, DOI: 10.1029/2006JC003807.

Barnston AG, Livezey RE. 1987. Classification, seasonality and persistence of low-frequency atmospheric circulation patterns. *Mon. Weather Rev.* **115**: 1083–1126.

Blackmon ML, Wallace JM, Lau N-C, Mullen SL. 1977. Observational study of Northern Hemisphere wintertime circulation. *J. Atmos. Sci.* **34**: 1040–1053.

Clinet S, Martin S. 1992. 700-HPA geopotential height anomalies from a statistical-analysis of the French Hemis data set. *Int. J. Climatol.* **12**: 229–256.

Dickson RR, Meincke J, Malmberg S, Lee A. 1988. The 'great salinity anomaly' in the northern North Atlantic 1968–1982. *Prog. Oceanogr.* **20**: 103–151.

Dickson RR, Osborne TJ, Hurrell JW, Meincke J, Blindheim J, Adlandsvik B, Vinje T, Alekseev G, Maslowski W. 2000. The Arctic Ocean response to the North Atlantic oscillation. *J. Climatol.* **13**: 2671–2696.

Doyle JD, Shapiro MA. 1999. Flow response to large-scale topography: the Greenland tip jet. *Tellus* **51A**: 728–748.

Haine TWN, Zhang S, Moore GWK, Renfrew IA. 2009. On the impact of high-resolution, high-frequency meteorological forcing on Denmark Strait ocean circulation. *Q. J. R. Meteorol. Soc.* **135**: 2067–2085.

Held IM, Ting M, Wang H. 2002. Northern winter stationary waves: theory and modeling. *J. Climatol.* **15**: 2125–2144.

Hoerling MP, Kumar A, Zhong M 1997. El Niño, La Niña, and the nonlinearity of their teleconnections. *J. Climatol.* **10**: 1769–1786.

Hurrell J, Kushnir Y, Ottersen G, Visbeck M. 2003. An overview of the North Atlantic oscillation. In *The North Atlantic Oscillation: Climatic Significance and Environmental Impact*, Hurrell J (ed.) 1–35, American Geophysical Union: Washington, DC.

Jones PD, Jonsson T, Wheeler D. 1997. Extension to the North Atlantic Oscillation using early instrumental pressure observations from Gibraltar and south-west Iceland. *Int. J. Climatol.* **17**: 1433–1450.

Kalnay E, Kanamitsu M, Kistler R, Collins W, Deaven D, Gandin L, Iredell M, Saha S, White G, Woollen J, Zhu Y, Leetmaa A, Reynolds R, Chelliah M, Ebisuzaki W, Higgins W, Janowiak J, Mo KC, Ropelewski C, Wang J, Jenne R, Joseph D. 1996. The NCEP/NCAR 40-year reanalysis project. *Bull. Amer. Meteorol. Soc.* **77**: 437–471.

Lavender KL, Davis RE, Owens WB. 2000. Mid-depth recirculation observed in the interior Labrador and Irminger seas by direct velocity measurements. *Nature* **407**: 66–69.

Marshall J, Dobson F, Moore GWK, Rhines P, Visbeck M, d'Asaro E, Bumke K, Chang S, Davis R, Fischer K, Garwood R, Guest P, Harcourt R, Herbaut C, Holt T, Lazier J, Legg S, McWilliams J, Pickart R, Prater M, Renfrew I, Schott F, Send U, Smethie W. 1998. The Labrador Sea deep convection experiment. *Bull. Amer. Meteorol. Soc.* **79**: 2033–2058.

Martin R, Moore GWK. 2007. Air–sea interaction associated with a Greenland reverse tip jet. *Geophys. Res. Lett.* **34**: L24802, DOI: 10.1029/2007GL031093.

Moore GWK. 2003. Gale force winds over the Irminger Sea to the east of Cape Farewell, Greenland. *Geophys. Res. Lett.* **30**: 1894, DOI: 10.1029/2003GL018012.

Moore GWK, Renfrew IA. 2005. Tip jets and barrier winds: a QuikSCAT climatology of high wind speed events around Greenland. *J. Climatol.* **18**: 3713–3725.

Murphy SJ, Washington R. 2001. United Kingdom and Ireland precipitation variability and the North Atlantic sea-level pressure field. *Int. J. Climatol.* **21**: 939–959.

Outten SD, Renfrew IA, Petersen GN. 2009. An easterly tip jet off Cape Farewell, Greenland. II: Simulations and dynamics. *Q. J. R. Meteorol. Soc.* **135**: 1934–1949.

Outten SD, Renfrew IA, Petersen GN. 2010. Erratum to 'An easterly tip jet off Cape Farewell, Greenland. II: Simulations and dynamics'. *Q. J. R. Meteorol. Soc.* **136**: 1099–1101.

Palmén E, Newton CW. 1969. *Atmospheric Circulation Systems: Their Structure and Physical Interpretation*. *International Geophysics Series*, Vol. 13. Academic Press: New York.

Petersen GN, Renfrew IA, Moore GWK. 2009. An overview of barrier winds off southeastern Greenland during the Greenland Flow Distortion experiment. *Q. J. R. Meteorol. Soc.* **135**: 1950–1967.

Pickart RS, Spall MA, Ribergaard MH, Moore GWK, Milliff RF. 2003. Deep convection in the Irminger Sea forced by the Greenland tip jet. *Nature* **424**: 152–156.

Pickart RS, Torres DJ, Fratantoni PS. 2005. The East Greenland Spill Jet. *J. Phys. Oceanogr.* **35**: 1037–1053.

Renfrew IA, Moore GWK, Guest PS, Bumke K. 2002. A comparison of surface layer and surface turbulent flux observations over the Labrador Sea with ECMWF analyses and NCEP reanalyses. *J. Phys. Oceanogr.* **32**: 383–400.

Renfrew IA, Moore GWK, Kristjansson JE, Olafsson H, Gray SL, Petersen GN, Bovis K, Brown PRA, Fore I, Haine T, Hay C, Irvine EA, Lawrence A, Ohigashi T, Outten S, Pickart RS, Shapiro M, Sproson D, Swinbank R, Woolley A, Zhang S. 2008. The Greenland flow distortion experiment. *Bull. Amer. Meteorol. Soc.* **89**: 1307–1324.

Renfrew IA, Outen SD, Moore GWK. 2009a. An easterly tip jet off Cape Farewell, Greenland. I: Aircraft observations. *Q. J. R. Meteorol. Soc.* **135**: 1919–1933.

Renfrew IA, Petersen GN, Sproson DAJ, Moore GWK, Adiwidjaja H, Zhang S, North R. 2009b. A comparison of aircraft-based surface-layer observations over Denmark Strait and the Irminger Sea with meteorological analyses and QuikSCAT winds. *Q. J. R. Meteorol. Soc.* **135**: 2046–2066.

Rodriguez-Puebla C, Encinas AH, Nieto S, Garmendia J. 1998. Spatial and temporal patterns of annual precipitation variability over the Iberian Peninsula. *Int. J. Climatol.* **18**: 299–316.

Sampe T, Xie SP. 2007. Mapping high sea winds from space: a global climatology. *Bull. Amer. Meteorol. Soc.* **88**: 1965–1978.

Seierstad IA, Stephenson DB, Kvamstø MG. 2007. How useful are teleconnection patterns for explaining variability in extratropical storminess? *Tellus* **59A**: 170–181.

Shabbar A, Higuchi K, Skinner W, Knox JL. 1997. The association between the BWA index and winter surface temperature variability over eastern Canada and west Greenland. *Int. J. Climatol.* **17**: 1195–1210.

Spall MA, Pickart RS. 2003. Wind-driven recirculations and exchange in the Labrador and Irminger Seas. *J. Phys. Oceanogr.* **33**: 1829–1845.

Spall MA, Price JF. 1998. Mesoscale variability in Denmark Strait: the PV outflow hypothesis. *J. Phys. Oceanogr.* **28**: 1598–1623.

Sproson DAJ, Renfrew IA, Heywood KJ. 2008. Atmospheric conditions associated with oceanic convection in the south-east Labrador Sea. *Geophys. Res. Lett.* **35**: L06601, DOI: 10.1029/2007GL032971.

Straneo F, Hamilton GS, Sutherland DA, Stearns LA, Davidson F, Hammill MO, Stenson GB, Rosing-Asvid A. 2010. Rapid circulation of warm subtropical waters in a major glacial fjord in East Greenland. *Nature Geosci.* **3**: 182–186.

Våge K, Pickart RS, Moore GWK, Ribergaard MH. 2008. Winter mixed layer development in the central irminger sea: the effect of strong, intermittent wind events. *J. Phys. Oceanogr.* **38**: 541–565.

Våge K, Pickart RS, Thierry V, Reverdin G, Lee CM, Petrie B, Agnew TA, Wong A, Ribergaard MH. 2009. Surprising return of deep convection to the subpolar North Atlantic Ocean in winter 2007–2008. *Nature Geosci.* **2**: 67–72.

Van den Dool HM, Peng P, Johansson A, Chelliah M, Shabbar A, Saha S. 2006. Seasonal-to-decadal predictability and prediction of North American climate: the Atlantic influence. *J. Climatol.* **19**: 6005–6024.

Wallace JM, Gutzler DS. 1981. Teleconnections in the geopotential height field during the Northern Hemisphere winter. *Mon. Weather Rev.* **109**: 784–812.

Woollings T, Hannachi A, Hoskins B. 2010. Variability of the North Atlantic eddy-driven jet stream. *Q. J. R. Meteorol. Soc.* **136**: 856–868.

Yashayaev I, Loder JW. 2009. Enhanced production of Labrador Sea Water in 2008. *Geophys. Res. Lett.* **36**: L01606, DOI: 10.1029/2008GL036162.


 